

GasPiRRaM: HSE's Gas Pipeline Decompression Model

Andrew P. L. Newton, Senior Scientist, Health and Safety Executive (HSE), Harpur Hill, Buxton, SK17 9JN, UK
andrew.newton@hse.gov.uk

As part of a programme of continuous development and improvement, the Health and Safety Executive (HSE) has identified the need for a new independent model for predicting the consequences of releases from major accident hazard pipelines transporting flammable and toxic gases. HSE requires a model that can predict the characteristics of pipeline releases from full-bore ruptures down to small holes. This paper introduces the Gas Pipeline Release Rate Model (GasPiRRaM) which has been developed to satisfy HSE's requirements for modelling gas releases.

GasPiRRaM follows the PolyPiRRaM derivation (Newton, 2024) but uses a numerical solution technique to enable its application to small holes. The model is conceptually analogous to PiRRaM (Newton, 2022) and the PipeBreak model (Webber et al., 1999) except a real gas equation of state is employed alongside an appropriate mass release rate model. The model smoothly transitions between full bore ruptures and holes without the need for calibration.

The model has been verified to analytical solutions, specifically the PolyPiRRaM model, in the full-bore rupture limit and the trivial exponential decaying vessel model in the small hole limit. A local sensitivity analysis was also performed to quantify the behaviour of the model predictions to input parameters and determine their respective importance. Finally, a series of model inter-comparisons has been undertaken to characterise the performance of GasPiRRaM in comparison to contemporary models.

A validation dataset has been assembled containing experiments using methane and air, across a range of scales (50 kg to 10,000 kg) and hole sizes (full bore rupture to small, 2% holes). GasPiRRaM performs acceptably well in comparison to these datasets.

The process of evaluating GasPiRRaM identified a new non-dimensionalisation scheme which collapses predictions corresponding to different hole sizes into a common behaviour. This provides important insights into the long-posed question about the transition between vessel and pipe behaviour in long pipelines and lays the foundations for a universal theory of pipeline transportation decompression.

The GasPiRRaM model has a wide range of applicability. The model recovers the expected behaviour in the limiting cases where analytical solutions exist. There are no unexpected sensitivities to input parameters and GasPiRRaM is found to make predictions that are quantitively and qualitatively similar to other pipeline decompression models. The model performs well, without need for calibration, for the full range of hole sizes where experimental data is available. Results of the GasPiRRaM testing demonstrate that the model is suitable for HSE's intended use cases.

Keywords: GasPiRRaM, MISHAP, HSE, pipeline modelling, holes, natural gas, hydrogen, MAH pipelines.

1 Introduction

This paper describes the new Gas Pipeline Release Rate Model (GasPiRRaM) which has been developed to provide transient characterisation of gas pipeline decompression for the Health and Safety Executive's (HSE) MISHAP computer model (Model for the estimation of Individual and Societal risk from HAzards of Pipelines). MISHAP is used to calculate the risks to people, and ultimately the land-use planning (LUP) zones from Major Accident Hazard (MAH) pipelines carrying flammable substances.

This paper briefly introduces the experimental data which is available to validate the model before reviewing the options available for modelling pipeline decompression. The quasi-steady compressible pipe-flow equations and other general principles of modelling transient pipeline releases are described, followed by an introduction to the approximate equation of state. The derivation of the model is then described, which starts with a series of calculations characterising the properties of a generalised expanding zone. Results from the expanding zone calculation are used to elicit solutions to the pipeline decompression problem. A discussion of the technical aspects of implementing the model is also provided.

Model testing is described, which includes verification to analytical results, and model intercomparisons. With assurances from the model testing activities that the model is accurately implemented, validation comparisons to a series of experiments releasing initially gaseous fluids are then performed. A discussion summarising the limitations and wider applicability of the new technique is presented.

2 Gas Pipeline Experiments

2.1 Overview

Pipeline experiments are useful to help inform the design of models as well as serving as a validation dataset. An extensive review of papers reporting experimental data was performed, with several experiments being identified as being suitable for validation purposes. These experiments generally consist of a pipe filled with a gas discharging through a single end, via either a valve opening or the explosive rupturing of a bursting disk. Depending on the objective of the experiment, instrumentation attached to the pipe may include pressure transducers, thermometers, and apparatus for inferring the mass of fluid remaining in the pipe. The experiments described hereafter form the validation dataset.

2.2 Nova Corporation of Alberta Field Measurements

Botros et al. (1989) present measurements from field experiments performed by the Nova Corporation of Alberta Field (NCAF). These relate to the depressurisation of a 25.5 km long, 203 mm diameter pipeline containing a natural gas mixture, through a vent stack with a cross-sectional area that was 25% of the main pipeline area, into an orifice with an area that is 17% of the pipe internal cross-sectional area . The initial pressure and temperature of the pipeline were 40.9 bar and 292 K, respectively. The material in the pipeline was a mixture of methane (91.6%), ethane (4.5%), nitrogen (1.8%) and propane (1.1%), with the remaining 1% being heavier hydrocarbons. The pressure was reported at the location immediately upstream of the vent stack.

2.3 Norris and Puls (1994)

Norris and Puls (1993) describe 15 gas releases, using three gas mixtures, from a reduced scale pipeline. The experimental pipeline was 609.6 m long with an internal diameter of 10.21 mm, and the experiments released gas through nozzles ranging from 2.4% to 100% of the pipe area. The experiments were designed to reproduce realistic length to diameter ratios. An equivalent full-scale pipe with an internal diameter of 150 mm would be approximately 9 km long. The inventory mass was measured, as were temperatures and pressures at different locations along the pipe. Norris and Puls (1994) includes plots of the mass flow rate against time that are easily digitised.

For small holes, the Norris and Puls (1993) data provides interesting insights into the characteristics of releases and serves as a useful validation dataset. However, for other releases, care must be taken to acknowledge the fact that the earliest stage of the release might not have been accurately captured. There are five experiments using air that are particularly useful for model validation purposes. These correspond to air initially stored at approximately 137 bar, with an assumed initial temperature of 5°C, released through holes of diameter 1.59 mm (1/16 inch), 3.18 mm (1/8 inch), and 10.21 mm (0.402 inch), corresponding to 2.4%, 9.7%, and 100% of the pipe cross-sectional area.

2.4 Alberta Petroleum Industry Trials

The Alberta Petroleum Industry Government Environmental Committee (APIGEC, 1979) undertook a series of studies aimed at evaluating the available techniques used to define potentially hazardous zones in the vicinity of sour gas operations (natural gas with a significant proportion of hydrogen sulphide). In all, 33 experiments were performed releasing high-pressure air using either a 4 km, long 157.18 mm inner diameter pipe, or a 7.1 km long, 304.84 mm inner diameter pipe, of which tabulated mass flow rate data is presented for 3 experiments.

The pipelines were buried with ruptures being triggered at the mid-point of the pipe, using a variety of different methods to examine the effect of cratering on the subsequent dispersion. Mass flow rates are estimated using a pressure measurement of the fluid in the pipe near the release point, and assuming that the flow was choked. The mass flow rate data presented corresponds to the flow from one side of the pipeline. This dataset forms a set of experiments that will be useful for validation of a pipeline decompression model.

2.5 Summary

Three experimental datasets have been identified (APIGEC, 1979; Botros et al., 1989; Norris and Puls, 1994) containing nine shock-tube type experiments that can be used to validate a pipeline decompression model. These experiments use either methane or air as the working fluid, with pipe lengths ranging from 600 m to 150 km, pressures ranging between 32 bar and 137 bar, hole sizes between 2.4% and 100% of the pipeline area, and pipe diameters covering 10 mm to 305 mm.

3 Gas Pipeline Decompression Literature

Historically, HSE has used the Bell-Bilio equation for basis of the LOSSP model, which has been examined to determine whether it is suitable for HSE's future requirements. The scientific basis of the Bell-Bilio equation is the Bell (1978) equation and to a lesser extent, the Wilson (1979 (Re-issued 1986)) model. The Bell equation is a phenomenological model which was derived in an informal manner, with no published verification or validation. The LOSSP model is an extension of the Bell (1978) equation, which is believed to allow for the modelling of asymmetrical pumped releases as well as releases through holes (what has previously been informally referred to as the HSE boundary conditions).

Since LOSSP was developed in the 1990s there have been significant developments in the understanding of modelling pipeline decompression. More experiments have been performed and new modelling techniques have been developed. Having identified limitations in the LOSSP model, and given that improved modelling techniques are available, a replacement model has been developed as part of HSE's continuous process of review and improvement.

There are various different techniques available to model pipeline decompression. These range from methods using computational fluid dynamics (CFD) techniques to solve the fully non-linear problem, such as OLGA, (Bendlksen et al., 1991) to integral type techniques used in other consequence models (the BLOWDOWN model in AspenTech's HYSYS software (Richardson & Saville, 1991), and GasPipe in DNV's Phast consequence model, Worthington (2022)). There are also techniques described in the literature which can be adapted to meet HSE's requirements. For example, Fannelop and Ryhming (1982) could be adapted by combining elements from the various rarefaction wave models (Eiber et al., 1993; Maxey, 1974). In addition, there are the older phenomenological models (Bell, 1978; Weiss et al., 1988; Wilson, 1979 (Re-issued 1986)), which offer the simplest possible option, but lack a robust theoretical foundation and justification. As this is the principal limitation of HSE's LOSSP tool, these type of models are precluded on the basis that they would not lead to a significant improvement in HSE's modelling capability.

Of the models identified, there are several potential methods that could be used to develop a new model. There is a significant range of modelling complexity ranging from very simple phenomenological models all the way up to CFD techniques. It would therefore be necessary to carefully balance the theoretical complexity and difficulty of implementation against model performance when considering a replacement for LOSSP. A novel recent development is the PolyPiRRaM tool (Newton, 2024). This method provides a framework for including real gas effects which can be hybridised with the PipeBreak/PiRRaM techniques enabling a robust method to be developed which can justifiably fulfil the HSE specification. Specifically, the PolyPiRRaM calculation can be re-derived relaxing some of the assumptions to enable the development of a tool capable of modelling releases through holes.

4 Governing Equations

The new model follows previous work in the field (Fannelop & Ryhming, 1982; Newton, 2022; Newton, 2024; Webber et al., 1999) in assuming that the momentum and energy conservation equations are slowly evolving, and that the convective acceleration is negligible (due to the absence of shocks significantly affecting the calculation). The equations describing the quasi-steady one-dimensional compressible flow along a pipe are given below for the mass, momentum, and energy conservation respectively:

$$\frac{\partial \rho}{\partial t} + \frac{\partial G}{\partial x} = 0, \qquad \frac{\partial P}{\partial x} = -\frac{2fG|G|v}{D_{\text{pipe}}} \qquad \text{and} \qquad h = \text{constant}. \tag{1}$$

Where ρ is the fluid density (kg m^{-3}), t is the time (s), G is the mass flux density ($\text{kg/m}^2\text{/s}$), v is the specific volume (m^3 kg^{-1}), x is the location along the pipe (m), P is the pressure (Pa), f is the Fanning friction factor (-), D_{pipe} is the pipe diameter (m) and h is the specific enthalpy (J/kg). In the new model, solutions to these equations are sought for horizontal and straight pipes containing fluids which are initially stationary with a uniform pressure along the pipe. These conditions are chosen to simplify the problem whilst also representing a justifiably conservative option.

The pipeline decompression is modelled as evolving through two flow regimes; an early time regime where the pipe has a stationary and expanding zone, and a late time regime where the entire contents of the pipe are in motion and the expanding zone fills the whole pipe. In this case the solutions derived in the next section can be adapted to represent each scenario through changing the limits of integration or by fixing the length of the expanding zone to be the pipe length. To mathematically describe the early and late time regimes, it is convenient to include a transition case which corresponds to the point at which the solution switches between the early and late time regimes. These different scenarios are shown in Figure 1 (overleaf), where blue indicates undisturbed stationary fluid at the initial pressure, and yellow to red represents the pressure change as the gas expands down the pipe (yellow and red corresponding to high and low pressure respectively).

The model derivation requires an approximate characterisation of the expanding zone, which is achieved via assuming power-law flow profiles. This algebraically links the mass flux density at the end of the pipe to the pressure profile in the expanding zone, the length of the expanding zone and its total mass. The early time regime then calculates the total pipe inventory as the sum of a stationary zone, with uniform density and pressure, and an expanding zone. The late time regime evaluates the expanding zone between the exit pressure and an upstream pressure which is less than the initial pressure. The transition case corresponds to the scenario where the length of the modelled expanding zone exactly matches the length of the pipe.

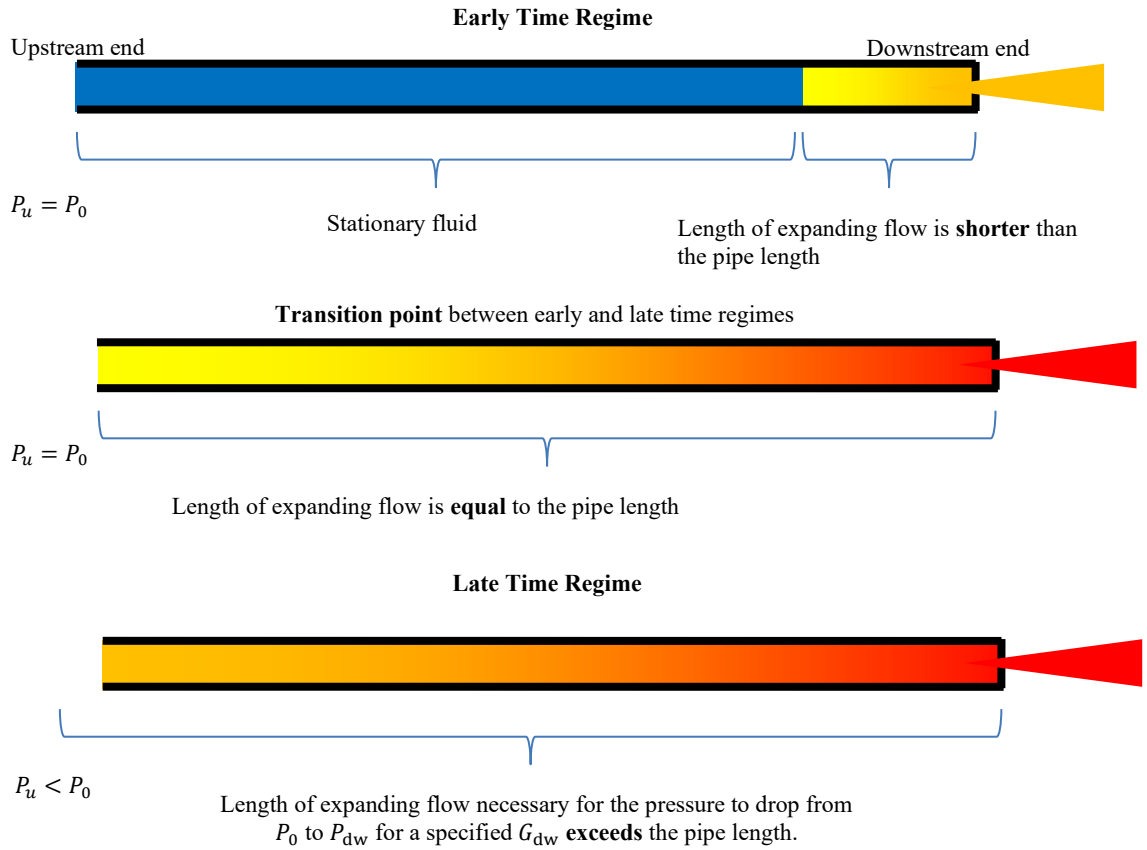

Figure 1 Schematic showing early time regime (top), the late time regime (bottom) and the transition point between them (middle).

5 Assumptions

5.1 Power Law Flow Profile

An axial co-ordinate system X^* is defined relative to the expanding zone such that $X^* = 0$ corresponds to the upstream end of the expanding zone, and $X^* = L_{\mathrm{expd}}$ corresponds to the point where the fluid leaves the pipe. This allows the following power-law profile to be assumed for the mass flux density in the expanding zone:

$$G(X^*, t) = \left(\frac{X^*}{L_{\mathrm{expd}}(t)}\right)^n G_{\mathrm{dw}}(t) \qquad (2)$$

Where $G_{\mathrm{d}}(t)$ is the time varying mass flux density of the fluid leaving the pipe (kg/m^2/s), X^* is the new co-ordinate relative to the expanding zone (m), L_{expd} is the length of the expanding zone (m) and n is the pipe flow index (-).

The pipe flow index is chosen using pre-existing values which have previously been used for pressure liquefied flow ($n = 0$, PipeBreak/PiRRaM) and expanding gas flows ($n = 2$, PHAST's GasPipe). The $n = 0$ value corresponds to a uniform mass flux density in the pipe, whereas $n = 2$ indicates a parabolic relationship between the mass flux density and its position in the expanding zone. Practically, these values along with the polytropic index (m) determine the average density in the expanding zone. Equation (2) has the property of being zero when $X^* = 0$ at the upstream end of the expanding zone, and matching the outlet mass flux density, $G\left(L_{\mathrm{expd}}(t), t\right) = G_{\mathrm{d}}(t)$, at the downstream end of the expanding zone. Except for the case when $n = 0$, where G is constant along the expanding section, which is used for modelling two-phase flows.

5.2 Polytropic Equation of State Modelling

A polytropic equation of state[1] relating the pressure and density of a fluid is assumed to have the following relationship:

$$\rho = \rho_0 \left(\frac{P}{P_0}\right)^m \tag{3}$$

Where P is the pressure (Pa), ρ is the fluid density (kg/m^3), and m is the polytropic index[2] (dimensionless). For gas initial conditions, the subscript 0 relates to stagnation conditions before the pipe is opened. Therefore, m is a constant which is found numerically to satisfy a momentum conservation integral. The above is therefore used as an approximation to an accurate equation of state that has the properties of matching the initial fluid density and satisfying an important momentum conservation integral which is introduced later.

The approach of approximating a real gas equation of state using polytropic equation of state to solve the quasi-steady compressible pipe flow equations was the key insight that underpins the success of the PolyPiRRaM model (Newton, 2024). Its application here enables the inventory to be accurately estimated using advanced equation of state modelling, without causing undue complexity in the modelling.

5.3 Mass Release Rate Modelling

To model releases through holes and punctures in pipes, it is necessary to predict the mass release rate of gas escaping confinement through holes. Using CoolProp (Bell et al., 2014) to perform real gas calculations, for methane and hydrogen as extreme limiting cases of materials that GasPiRRaM is expected to model, it was found that there is no benefit for using real gas modelling for hydrogen, and methane could be modelled with acceptable accuracy assuming that the pressure remains below 100 bar.

Given that UK natural gas pipelines operate at pressures below 100 bar[3], and that the temperature typically assumed by HSE in pipeline modelling is 5°C, there is no requirement to adopt real gas modelling. GasPiRRaM therefore uses ideal gas modelling with a unitary coefficient of discharge. This is a reasonable and slightly cautious assumption when the flow is choked.

5.4 Expanding Zone Solution

The polytropic approximation (3) and the assumed mass flux density profile (2) are substituted into the momentum conservation equation (1). The resulting equation is integrated from an arbitrary position in the expanding zone ($X^* = X$) to the end of the pipe ($X^* = L_{\text{expd}}$), which corresponds to the pressure between $P(X)$ and $P_{\text{dw}} = P\left(L_{\text{expd}}\right)$. Noting that $G_{\text{dw}} > 0$ (i.e. velocity in the positive X^* direction the following relationship is obtained:

$$\frac{\rho_{\text{up}}}{P_{\text{up}}^m} \int_{P(X)}^{P_{\text{dw}}} P^m dP = -\frac{2f}{D_{\text{pipe}}} \frac{G_{\text{dw}}^2}{L_{\text{expd}}^{2n}} \int_{X}^{L_{\text{expd}}} X^{*2n}\, dX^* \tag{4}$$

This is integrated to get the following expression for the pressure at a location X in the expanding zone:

$$P(X)^{m+1} - P_{\text{dw}}^{m+1} = P_{\text{up}}^m \frac{m+1}{\rho_{\text{up}}} \frac{2fG_{\text{dw}}^2}{D_{\text{pipe}}} \frac{m+1}{2n+1} L_{\text{expd}} \left[1 - \left(\frac{X}{L_{\text{expd}}}\right)^{2n+1}\right] \tag{5}$$

Setting $X = 0$ and $\mathrm{P}(X^* = 0) = P_{\text{up}}$, the length of the expanding zone is given by:

$$P_{\text{up}}^{m+1} - P_{\text{dw}}^{m+1} = \frac{P_{\text{up}}^m 2fG_{\text{dw}}^2}{\rho_{\text{up}} D_{\text{pipe}}} \frac{m+1}{2n+1} L_{\text{expd}} \tag{6}$$

Which is re-arranged to:

---

[1] See the footnote in Landau and Lifschitz, (1991) on page 318: *"The name polytropic is derived from polytropic process, i.e. one in which the pressure varies as some power of volume"*.

[2] Here, the polytropic index (m) is defined for convenience via $\rho = \rho_0 (P P_0^{-1})^m$(3). This is similar to other authors who define m to relate pressure (P) and volume (V) during a process via $PV^m = C$ where C is a constant, which corresponds to a slightly different relationship: $P = P_0 (\rho \rho_0^{-1})^m$.

[3] Z. Chaplin Private Communication, 2025

$$L_{\text{expd}} = \frac{\rho_{\text{up}} D_{\text{pipe}}}{2 f G_{\text{dw}}^2 P_{\text{up}}^m} \frac{2n+1}{m+1} \left(P_{\text{up}}^{m+1} - P_{\text{dw}}^{m+1}\right) \tag{7}$$

This matches the PolyPiRRaM calculation, though PolyPiRRaM takes the limiting case $P_{\text{up}}^{m+1} \gg P_{\text{dw}}^{m+1} \to 0$. Using the polytropic equation of state to substitute the density (ρ_0), the length of the expanding zone is given as:

$$L_{\text{expd}} = \frac{\rho_0 D_{\text{pipe}}}{P_0^m 2 f G_{\text{dw}}^2} \frac{2n+1}{m+1} \left(P_{\text{up}}^{m+1} - P_{\text{dw}}^{m+1}\right) \tag{8}$$

Which conveniently rearranges to provide the upstream pressure:

$$P_{\text{up}} = \left[P_{\text{dw}}^{m+1} + L_{\text{expd}} \left(\frac{\rho_0 D_{\text{pipe}}}{P_0^{\text{m}} 2 f G_{\text{dw}}^2} \frac{2n+1}{m+1} \right)^{-1} \right]^{\frac{1}{m+1}} \tag{9}$$

The pressure profile (5) in the pipe therefore becomes:

$$P(X) = \left\{ {P_{\text{dw}}}^{m+1} + \left(P_{\text{up}}^{m+1} - P_{\text{dw}}^{m+1}\right) \left[1 - \left(\frac{X^*}{L_{\text{expd}}} \right)^{2n+1} \right] \right\}^{\frac{1}{m+1}} \tag{10}$$

Equation (5) also allows the mass in the expanding zone (M_{expd}) to be calculated as the integral of density over its length. Using the approximate polytropic equation of state (3), the mass in the expanding zone is given by:

$$\begin{aligned} \frac{M_{\text{expd}}}{A_{\text{pipe}}} &= \int_0^{L_{\text{expd}}} \rho\left(P(X^*)\right) dX^* \\ &= \int_0^{L_{\text{expd}}} \frac{\rho_{\text{up}}}{P_{\text{up}}^m} \left\{ {P_{\text{dw}}}^{m+1} + \left(P_{\text{up}}^{m+1} - P_{\text{dw}}^{m+1}\right) \left[1 - \left(\frac{X^*}{L_{\text{expd}}} \right)^{2n+1} \right] \right\}^{\frac{\text{m}}{m+1}} dX^* \end{aligned} \tag{11}$$

Which, with a change of variable, $x^* = \frac{X^*}{L_{\text{expd}}}$, becomes:

$$\begin{aligned} \frac{M_{\text{expd}}}{L_{\text{expd}} A_{\text{pipe}} \rho_{\text{up}}} &= \frac{\bar{\rho}}{\rho_{\text{up}}} \\ &= \int_0^1 \frac{1}{P_{\text{up}}^m} \left\{ {P_{\text{dw}}}^{m+1} + \left(P_{\text{up}}^{m+1} - P_{\text{dw}}^{m+1}\right) \left[1 - \left(\frac{X^*}{L_{\text{expd}}} \right)^{2n+1} \right] \right\}^{\frac{\text{m}}{m+1}} dx^* \\ &= \int_0^1 \left\{ \frac{P_{\text{dw}}^{m+1}}{P_{\text{up}}^{m+1}} + \left(1 - \frac{P_{\text{dw}}^{m+1}}{P_{\text{up}}^{m+1}} \right) \left[1 - {x^*}^{2n+1} \right] \right\}^{\frac{\text{m}}{m+1}} dx^* \end{aligned} \tag{12}$$

Where $\bar{\rho}$ is the average density in the expanding zone. This is simplified by defining the dimensionless constant $\lambda = \frac{P_{\text{dw}}^{m+1}}{P_{\text{up}}^{m+1}}$:

$$\frac{M_{\text{expd}}}{L_{\text{expd}} A_{\text{pipe}} \rho_{\text{up}}} = \int_0^1 \left\{ \lambda + (1-\lambda) \left[1 - {x^*}^{2n+1} \right] \right\}^{\frac{\text{m}}{m+1}} dx^* \tag{13}$$

Expanding the brackets within the integral:

$$\frac{M_{\text{expd}}}{L_{\text{expd}} A_{\text{pipe}} \rho_{\text{up}}} = \int_0^1 \left\{ \lambda + (1-\lambda) - (1-\lambda)\, {x^*}^{2n+1} \right\}^{\frac{\text{m}}{m+1}} dx^* \tag{14}$$

Further simplifying:

$$\frac{M_{\text{expd}}}{L_{\text{expd}} A_{\text{pipe}} \rho_{\text{up}}} = \int_0^1 \left\{ 1 - (1-\lambda)\, {x^*}^{2n+1} \right\}^{\frac{\text{m}}{m+1}} dx^* \tag{15}$$

Extracting the factor $(1-\lambda)^{\frac{m}{m+1}}$ to outside the integral and collecting like terms gives:

$$\frac{M_{\text{expd}}}{L_{\text{expd}}A_{\text{pipe}}\rho_{\text{up}}} = (1-\lambda)^{\frac{m}{m+1}}\int_0^1 \left(\frac{1}{1-\lambda} - x^{*2n+1}\right)^{\frac{m}{m+1}} dx^* \tag{16}$$

Which is simplified further using $\mu = \frac{1}{1-\lambda}$, $\omega = 2n+1$, and $\psi = \frac{m}{m+1}$:

$$\frac{M_{\text{expd}}}{L_{\text{expd}}A_{\text{pipe}}\rho_{\text{up}}} = (1-\lambda)^{\psi} I \tag{17}$$

Where the key integral (I) to be evaluated is:

$$I = \int_0^1 (\mu - x^{*\omega})^{\psi}\, dx^* \tag{18}$$

Choosing the substitution $u = x^{*\omega}$, which corresponds to $du = \omega x^{*\omega-1}dx^*$ or $dx^* = \frac{1}{\omega}x^{*1-\omega}du = \frac{1}{\omega}u^{\frac{1-\omega}{\omega}}du$ and leaves the limits unchanged:

$$I = \frac{1}{\omega}\int_0^1 (\mu - u)^{\psi}\, u^{\frac{1}{\omega}-1} du \tag{19}$$

A further substitution of $u = \mu s$, which corresponds to $du = \mu ds$, changes the limits of integration:

$$I = \frac{1}{\omega}\int_0^{\mu^{-1}} (\mu - \mu s)^{\psi}\, (\mu s)^{\frac{1}{\omega}-1} \mu ds \tag{20}$$

Collecting constants reveals the following expression:

$$I = \frac{\mu^{\psi+\frac{1}{\omega}}}{\omega}\int_0^{\mu^{-1}} s^{\frac{1}{\omega}-1}(1-s)^{\psi} ds \tag{21}$$

Which is alternatively expressed[4] as the incomplete beta function:

$$I = \frac{\mu^{\frac{\psi\omega+1}{\omega}}}{\omega}\mathrm{B}_{\mu^{-1}}\left(\frac{1}{\omega}, \psi+1\right) \tag{22}$$

The mass in the expanding zone (M_{expd}) is therefore given by:

$$M_{\text{expd}} = L_{\text{expd}}A_{\text{pipe}}\rho_{\text{up}}(1-\lambda)^{\psi}\frac{\mu^{\frac{\psi\omega+1}{\omega}}}{\omega}\mathrm{B}_{\mu^{-1}}\left(\frac{1}{\omega}, \psi+1\right) \tag{23}$$

Where:

$$\mu = \frac{1}{1-\lambda} = \frac{P_{\text{up}}^{m+1}}{P_{\text{up}}^{m+1} - P_{\text{dw}}^{m+1}} \tag{25}$$

Which allows a further simplification:

$$M_{\text{expd}} = \frac{1}{\omega}L_{\text{expd}}A_{\text{pipe}}\rho_{\text{up}}\left(\frac{P_{\text{up}}^{m+1}}{P_{\text{up}}^{m+1} - P_{\text{dw}}^{m+1}}\right)^{\frac{1}{\omega}}\mathrm{B}_{\mu^{-1}}\left(\frac{1}{\omega}, \psi+1\right) \tag{26}$$

[4] The incomplete beta function is given by:

$$\mathrm{B}_z(p,q) = \int_0^z s^{p-1}(1-s)^{q-1} ds$$

Choosing $z = 1$ returns the complete integral of the beta function.

Considering the limiting case as $\lambda \to 0$ (i.e. $P_{\mathrm{up}}^{m+1} \gg P_{\mathrm{dw}}^{m+1}$), noting the special properties[5] of the gamma function, gives:

$$\lim_{\lambda \to 0} \frac{M_{\mathrm{expd}}}{L_{\mathrm{expd}} A_{\mathrm{pipe}} \rho_{\mathrm{up}}} \to \frac{1}{\omega} \mathrm{B}_1 \left(\frac{1}{\omega}, \psi + 1\right) = \frac{\Gamma\left(1 + \frac{1}{2n+1}\right) \Gamma\left(1 + \frac{m}{m+1}\right)}{\Gamma\left(1 + \frac{m}{m+1} + \frac{1}{2n+1}\right)} \tag{28}$$

therein recovering the expected PolyPiRRaM result, which is derived for the case where the downstream pressure is assumed to be negligible in comparison to the upstream pressure.

6 Pipe Flow Calculation

6.1 Solution Time Stepping

The solution method closely follows the PipeBreak/PiRRaM approach in that the mass flow rate is iteratively reduced from the initial mass flow rate (M_0,kg s^{-1}), to a series of smaller values ($\dot{M}_i$,kg s^{-1}) at step i. For each later mass flow rate, the inventory is calculated using the appropriate calculation for either the early or late time regime respectively. This results in a list of paired values for the mass flow rate and the inventory mass $\left(\dot{M}_{\mathrm{pipe},i}, M_{\mathrm{pipe},i}\right)$ from which the timing of each step can be easily inferred using the trapezium rule for the integral $dt = \frac{dM}{\dot{M}}$:

$$t_{i+1} = t_i + \frac{1}{2}\left(M_{\mathrm{pipe},i+1} - M_{\mathrm{pipe},i}\right)\left(\frac{1}{\dot{M}_{\mathrm{pipe},i+1}} + \frac{1}{\dot{M}_{\mathrm{pipe},i}}\right) \tag{29}$$

6.2 Early Time Regime

In the early time regime, the mass in the pipe at step i, is given by:

$$M_{\mathrm{pipe},i} = A_{\mathrm{pipe}}\left(L_{\mathrm{pipe}} - L_{\mathrm{expd},i}\right)\rho_0 + M_{\mathrm{expd},i}$$

Where the mass in the expanding zone is calculated using the pipe exit pressure ($P_{\mathrm{dw},i}$, Pa), which is in turn given by the mass flow rate ($\dot{M}_i$, kg s^{-1}).

6.3 Late Time Regime

If the length of the expanding zone exceeds the pipe length, the expanding zone fills the pipe. In this case, the upstream pressure (P_{up}, Pa) is calculated using the equation for the length of the expanding zone (7) upon setting $L_{\mathrm{expd}} = L_{\mathrm{pipe}}$ as:

$$P_{\mathrm{up}} = \left(P_{\mathrm{dw}}^{m+1} + \frac{2 f L_{\mathrm{pipe}} G_{\mathrm{dw}}^2 P_{\mathrm{up}}^m}{P_{\mathrm{up}} \rho_{\mathrm{up}} D_{\mathrm{pipe}}} \frac{m+1}{2n+1}\right)^{\frac{1}{m+1}} \tag{30}$$

This can then be used in the expanding zone mass calculation, which is evaluated again with $L_{\mathrm{expd}} = L_{\mathrm{pipe}}$.

6.4 Overview of the Solution Method

The GasPiRRaM calculation is analogous to the PiRRaM/PipeBreak model, and is summarised as follows:

1. Compute the initial mass flow rate using the isentropic ideal gas choked flow equations with a unitary coefficient of discharge
2. Calculate initial mass using CoolProp
3. Calculate the polytropic index (m) using the PolyPiRRaM calculation. The pipeline calculation is performed using an appropriate value of m. As there is no benefit to using real gas model for mass release rate modelling for the cases being considered, ideal gas modelling is used to predict the mass release rate
4. Begin loop
    a. Reduce the exit mass flow rate by some factor (taken to be 0.95)
    b. Calculate the pressure immediately upstream of the end of the pipe corresponding to the given mass flow rate

[5] The Gamma function $\Gamma(z)$ satisfies: $\Gamma(z+1) = z\Gamma(z)$.

c. Calculate the length of the expanding zone
    i. Calculate the upstream pressure if expanding zone length exceeds the length of the pipe
d. Using the expanding zone length, calculate the inventory of the pipe
e. Calculate the time corresponding to new step
f. Store required data
g. Return to step 4a until the until desired time is achieved

5. Process final data to produce model results.

7 Model Testing

7.1 Comparison to Analytical Solutions

There are two limiting cases where the equations describing the pipeline decompression are analytically tractable. The first corresponds to decompression through a full bore rupture where the PolyPiRRaM solution can be used (Newton, 2024), and the second corresponds to the small hole limit where the pipeline behaves like a vessel and an exponential decay model is appropriate[6] (Bell, 1978). To enable a convenient comparison of the GasPiRRaM results across the range of hole sizes, predictions are plotted using normalised mass flow rate ($\dot{M}^*$,-) and time (t^*,-) which are defined via:

$$\dot{M}^* = \frac{\dot{M}(t)}{\dot{M}_0} \quad \text{and} \quad t^* = \frac{M_0}{\dot{M}_0} t \tag{31}$$

Figure 2 shows the GasPiRRaM mass flow rate predictions for a range of hole sizes, normalised using the basic scheme (31). The GasPiRRaM and PolyPiRRaM predictions are indistinguishable in the full-bore rupture limit, which is excellent confirmation that the GasPiRRaM model is implemented accurately. As the hole size decreases, the model continuously transitions to becoming very close to the vessel model, which models the release as an isothermal ideal gas without friction. As GasPiRRaM includes real gas effects, minor differences between the vessel model and GasPiRRaM are acceptable. The agreement between the two models is sufficiently close to be sure that the GasPiRRaM model is working as intended.

A different non-dimensionalisation is possible using the time, mass and mass flow rate corresponding to the transition between the early and late time regimes (t_{trans}, M_{trans} and $\dot{M}_{\text{trans}}$ respectively). These are calculated just at the point where the expanding zone fills the pipe for the first time. New dimensionless time and mass variables (M^{**},-; t^{**},-) are defined in terms of the characteristics of the pipe at the transition time (t_{trans}) using:

$$M^{**} = \frac{M(t)}{M_{\text{trans}}} \text{ and } t^{**} = 1 + \frac{M_{\text{trans}}}{\dot{M}_{\text{trans}}}(t - t_{\text{trans}}) \tag{32}$$

The new time variable is chosen such that $t^{**} = 1$ corresponds to the precise point of switching between the early and late time regimes. This is necessary to highlight the dimensional collapse of the model prediction. Consequently, the starting times of the different model predictions are chosen to ensure that all the models reach the transition point at the same dimensionless time ($t^* = 1$). Figure 3 shows the GasPiRRaM predictions plotted using the new non-dimensionalisation (32), which shows an excellent collapse of the experimental predictions in the new dimensionless space.

Identifying nondimensionalisation schemes is an important element of modelling, as it can highlight deficiencies and weaknesses in the models. The nondimensionalisation scheme (32) devised above enables a new insight into pipeline modelling, especially in relation to extending PolyPiRRaM to releases through holes. Newton (2025) exploits this observation deriving PolyPiRRaM+, a universal model of compressible pipeline decompression that can be applied to gas and two-phase releases.

[6] The exponentially decaying ideal gas vessel decompression model is easily derived assuming: 1) isentropic choked flow; and 2) that the contents of the vessel are isothermal during the decompression. The transient mass flow then takes the form $\dot{M} = \dot{M}_0 e^{-\frac{\dot{M}_0}{M_0} t}$.

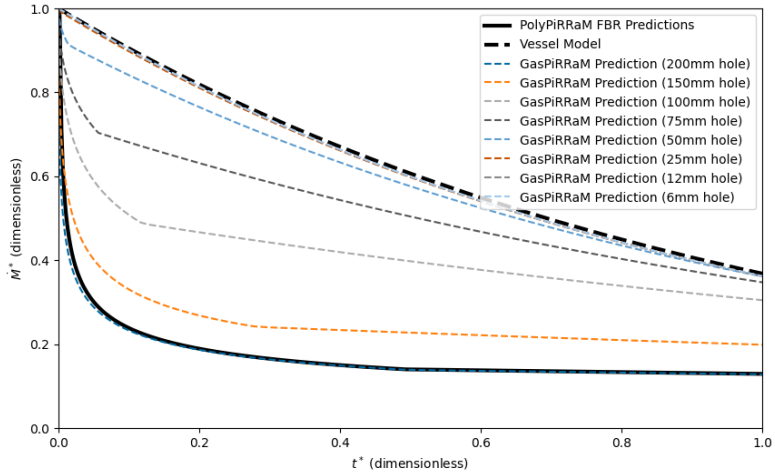

Figure 2 GasPiRRaM predictions of the mass flow rate vs time, presented using dimensionless variables for a range of hole sizes between 200 mm and 6 mm. Also shown are predictions corresponding to the analytically tractable limiting cases of full-bore rupture (PolyPiRRaM, solid black line) and the vessel case (dashed black line).

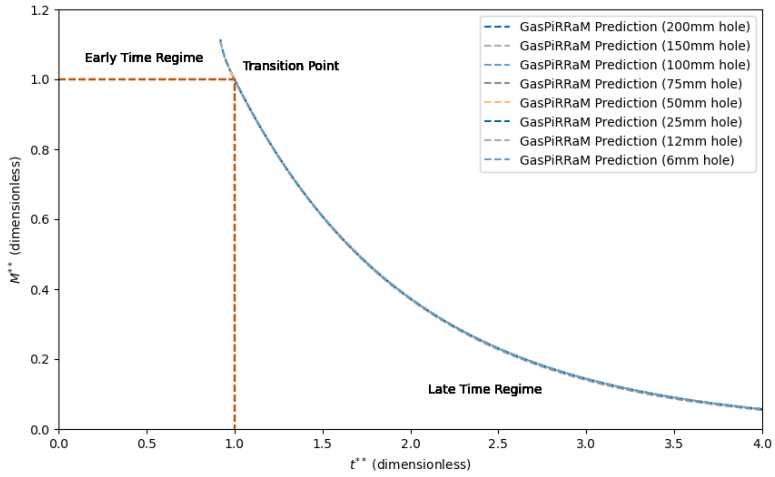

Figure 3 GasPiRRaM predictions of the mass flow rate vs time, for a range of hole sizes between 200 mm and 6 mm plotted using t^{**} and M^{**}. The early and late time regimes are indicated as $t^{**} < 1$ and $t^{**} > 1$ respectively, with the transition point occurring at $t^{**} = 1$

7.2 Comparison to DNV's PHAST GasPipe: Full-Bore Ruptures

GasPiRRaM predictions have been compared to DNV PHAST's GasPipe model using the parameters given in Table 1 corresponding to a full-bore rupture of a pipeline transporting either methane or hydrogen.

Table 1 GasPiRRaM input conditions for the full-bore rupture cases presented in Figure 4

Material	$D_{\mathbf{pipe}}$	$D_{\mathbf{hole}}$	$A_{\mathbf{hole}}A_{\mathbf{pipe}}^{-1}$	$L_{\mathbf{pipe}}$	P_0	T_o	μ
Methane	870 mm	870 mm	100%	8 km	100 bar	20 °C	45×10^{-6} m
Hydrogen	150 mm	150 mm	100%	16 km	100 bar	15 °C	45×10^{-6} m

Figure 4 presents predictions from both models for the methane case (left) and the hydrogen case (right). GasPiRRaM predictions are shown using the orange line, and PHAST GasPipe predictions are shown using blue lines. The agreement between the models in both cases is excellent. The GasPiRRaM model slightly under predicts the GasPipe mass flow rate during the first few seconds, however, the duration and magnitude of the difference is small and not considered to be of practical significance.

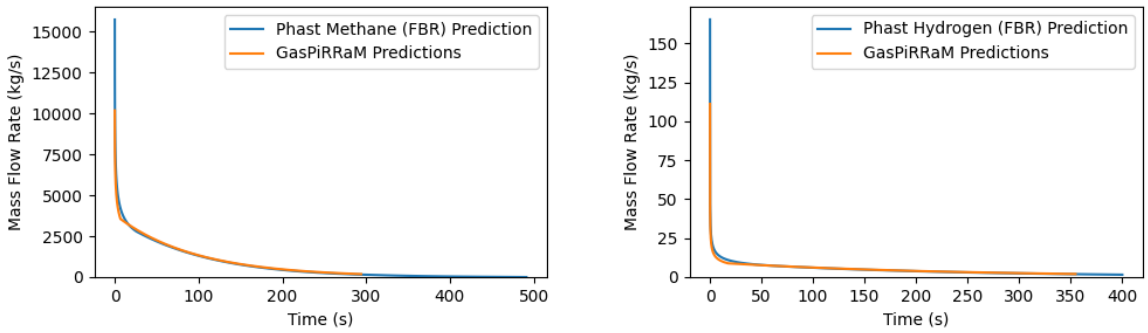

Figure 4 Plots showing a comparison of the transient mass flow rate from GasPiRRaM and PHAST V9.0 for full bore ruptures to pipelines containing methane (left) and hydrogen (right). GasPiRRaM predictions are shown using orange lines, and experimental measurements are shown using blue lines.

7.3 Comparison to GasPipe in DNV's PHAST for Hole Releases (Hydrogen)

GasPiRRaM predictions have been compared to DNV PHAST's GasPipe model using the parameters given in Table 2 corresponding to releases through holes for a pipeline transporting hydrogen.

Table 2 GasPiRRaM input conditions for the full-bore rupture cases presented in Figure **4**5

Material	$D_{\mathbf{pipe}}$	$D_{\mathbf{hole}}$	$A_{\mathbf{hole}}A_{\mathbf{pipe}}^{-1}$	$L_{\mathbf{pipe}}$	P_0	T_o	μ
Hydrogen	150 mm	75 mm	25%	16 km	100 bar	15 °C	45×10^{-6} m
Hydrogen	150 mm	50 mm	11.1%	16 km	100 bar	15 °C	45×10^{-6} m

Figure 5 is a plot of mass flow rate predictions from the two models, for the 75 mm hole (left) and 50 mm hole (left) using the same colouring convention as used previously (GasPiRRaM and PHAST predictions are coloured orange and blue respectively). The agreement between the models is excellent. As with the full-bore rupture releases, it is notable that the initial GasPiRRaM predicted mass flow rate is slightly lower during the first few seconds of the releases, though the later stages are almost identical.

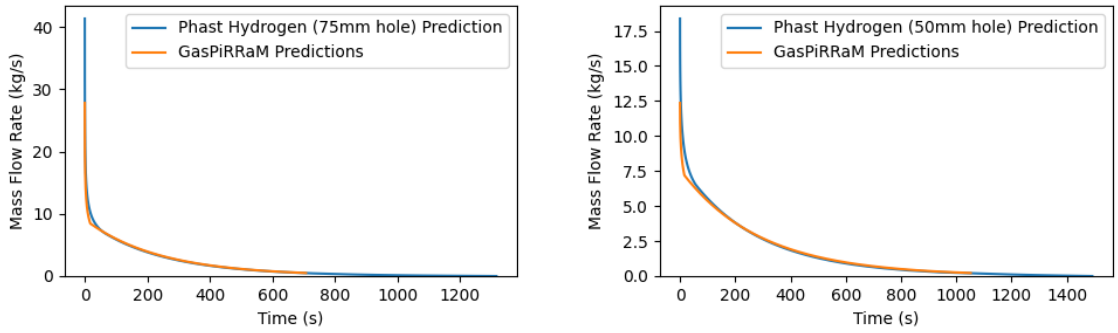

Figure 5 Plots showing a comparison of the transient mass flow rate from GasPiRRaM and PHAST V9.0 for a 25% (left) and 11% (right) hole to a pipeline containing hydrogen. GasPiRRaM predictions are shown using orange lines, and PHAST predictions are shown using blue lines.

Hole Releases (Methane)

GasPiRRaM predictions are compared to DNV PHAST's GasPipe model using the parameters given in Table 3, corresponding to releases through holes for a pipeline transporting methane. Figure 6 plots the transient mass flow rates predicted by GasPipe (Phast) for the 21% hole (left) and 5.3% hole (right). Qualitatively the agreement between the two model predictions is very similar, although the GasPipe model does predict noticeably higher initial mass flow rates.

The agreement between GasPiRRaM and Phast for the methane releases is not as close for methane as it was the hydrogen comparisons. The reason for which is likely due to the different pipe diameters and exit plane velocities causing friction to be less important in the methane release and be more significant in the hydrogen release. Re-running the comparisons for methane using a longer narrower pipe shows significantly improved agreement between GasPiRRaM and Phast. The GasPipe technical documentation (Worthington, 2022) indicates that the validity of GasPipe is expected to be better for large

aperture fraction, becoming less accurate for aperture fractions less than 20%. In Section 7.1 GasPiRRaM was shown to match the vessel models in the limiting case of arbitrarily small holes, in which case, the GasPiRRaM is likely to be more reliable in the small hole limit, though it is important to note that GasPipe has modelling capabilities that are not included in GasPiRRaM such a modelling the effect of pumping, non-uniform initial conditions, and value closure.

Table 3 GasPiRRaM input conditions for the full-bore rupture cases presented in Figure **4**6

Material	$D_{\mathbf{pipe}}$	$D_{\mathbf{hole}}$	$A_{\mathbf{hole}}A_{\mathbf{pipe}}^{-1}$	$L_{\mathbf{pipe}}$	P_0	T_o	μ
Methane	870 mm	400 mm	21%	8 km	100 bar	20 °C	45 um
Methane	870 mm	200 mm	5.3%	8 km	100 bar	20 °C	45 um

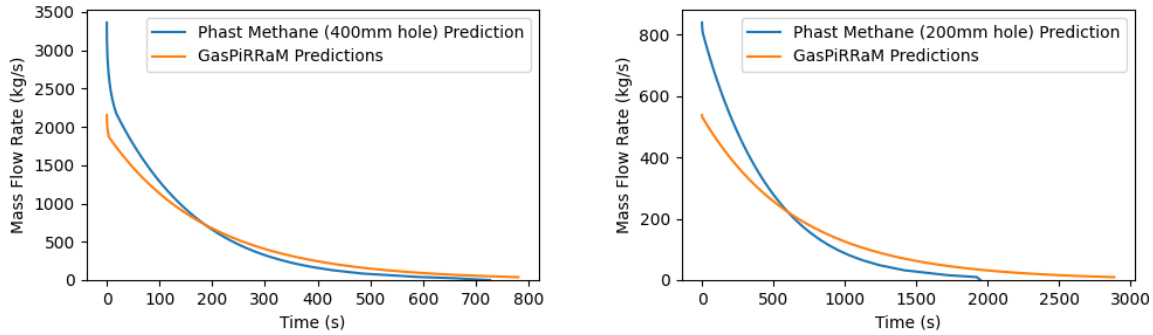

Figure 6 Plots showing a comparison of the transient mass flow rate from GasPiRRaM and PHAST V9.0 for a 21% (left) and 5.3% (right) hole to a pipeline containing methane. GasPiRRaM predictions are shown using orange lines, and Phast predictions are shown using blue lines.

7.4 Comparisons to FRED

GasPiRRaM predictions are compared to the long pipeline model in Shell FRED, distributed by GEXCON (Betteridge, 2023) for a full-bore rupture to a methane pipeline using the parameters given in Table 4.

Table 4 GasPiRRaM input conditions for the full-bore rupture cases presented in Figure **4**7.

Material	$D_{\mathbf{pipe}}$	$D_{\mathbf{hole}}$	$A_{\mathbf{hole}}A_{\mathbf{pipe}}^{-1}$	$L_{\mathbf{pipe}}$	P_0	T_o	μ
Methane	870 mm	870 mm	100%	8 km	100 bar	20 °C	45 um

Figure 7 shows a comparison of the mass flow rate vs time for predictions from GasPiRRaM and FRED using orange and blue lines respectively. Whilst the predictions are not quantitively identical, they are qualitatively very similar and capture the decay in the mass flow rate very reasonably.

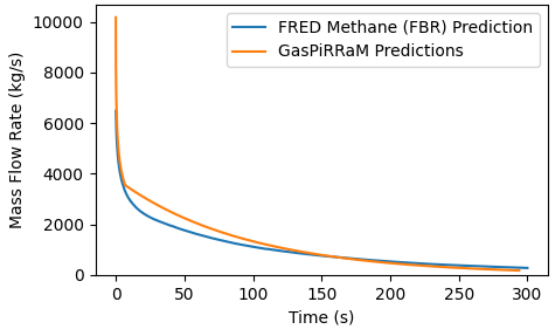

Figure 7 Plots showing a comparison of the transient mass flow rate from GasPiRRaM and FRED for full bore ruptures of pipelines containing methane. GasPiRRaM predictions are shown using orange lines, and FRED predictions are shown using blue lines.

8 Validation

8.1 Norris and Puls (1993) Experiments

Norris and Puls (1993) describe 15 gas releases, using three gas mixtures, from a reduced scale pipeline. The experimental pipeline was 609.6 m long with an internal diameter of 10.2 mm. Of interest to this study are the experiments releasing air initially stored at 138 bar and 20 °C, through nozzles ranging from 2.4% to 100% of the pipe area. The experiments were designed to reproduce realistic length to diameter ratios. An equivalent full-scale pipe with an internal diameter of 150 mm would be approximately 9 km long. GasPiRRaM predictions for these experiments are generated using the input parameters described in Table 5 below. Notably, air is modelled using nitrogen as a proxy substance.

Table 5 GasPiRRaM model input parameters corresponding to the Norris and Puls (1993) dataset

Material	$D_{\mathbf{pipe}}$(mm)	$D_{\mathbf{hole}}$(mm)	$A_{\mathbf{hole}}A_{\mathbf{pipe}}^{-1}$	$L_{\mathbf{pipe}}$(m)	P_0(bar)	T_o(°C)	μ(um)
Nitrogen	10.2	10.2	FBR†	609.6	138	20	45
Nitrogen	10.2	7.14	50†† %	609.6	138	20	45
Nitrogen	10.2	4.76	25†† %	609.6	138	20	45
Nitrogen	10.2	3.175	10†† %	609.6	138	20	45
Nitrogen	10.2	1.58	2.5†† %	609.6	138	20	45

† Full bore rupture

†† Percentage fractional areas as reported in Norris and Puls.

Figure 8 (overleaf) compares GasPiRRaM predictions for the mass flow rate (orange line) against the experimental data (blue line) for the full-bore rupture (top left), 50% hole (top right), 25% hole (middle row left), 10% (middle row right), and 2.5% hole (bottom row). Across all the plots the agreement between the model prediction and the experimental data is excellent. The apparently over prediction in mass flow rate corresponds to a rapid change in mass flow rate, and corresponding small change in inventory, during the early time regime when both stationary and expanding zones are present in the pipe. For gas releases, the mass releases during the early time regime is small in comparison to the total inventory so it is not easily discernible from the inventory measurements, though it is present in the exit pressure measurements which are not reported here for brevity.

8.2 APIGEC (1979) Experiments

The Alberta Petroleum Industry Government Environmental Committee (APIGEC, 1979) undertook a series of studies aimed at evaluating the available techniques used to define potentially hazardous zones in the vicinity of sour gas operations (natural gas with a significant proportion of hydrogen sulphide). In all, 33 experiments were performed releasing high-pressure air using either a 4 km long 157.18 mm inner diameter[7] pipe; or a 7.1 km long 304.84 mm inner diameter[8] pipe, of which tabulated mass flow rate data is presented for three full bore rupture experiments.

The pipelines were buried with ruptures being triggered at the mid-point of the pipe, using a variety of different methods, to examine the effect of cratering on the subsequent dispersion. Mass flow rates are estimated using a pressure measurement of the fluid in the pipe near the release point, and assuming that the flow is choked. The mass flow rate data presented corresponds to the flow from one side of the pipeline.

GasPiRRaM predictions for these experiments were generated using the input parameters described in Table 6 below. Notably, air was modelled using nitrogen as a proxy substance.

[7] 168.3 mm outer diameter with a 5.56 mm wall thickness.

[8] 323.9 mm outer diameter with a 9.53 mm wall thickness

Table 6 GasPiRRaM model input parameters corresponding to the API dataset

Case	Material	D_{pipe} (mm)	D_{hole} (mm)	$A_{hole}A_{pipe}^{-1}$	L_{pipe} (km)	P_0 (bar)	T_o (°C)	μ (um)
API1	Nitrogen	168	168	100%	2	71	5	45
API2	Nitrogen	168	168	100%	2	36	5	45
API3	Nitrogen	300.5	300.5	100%	3.55	71	5	45

Figure 9 shows comparisons of GasPiRRaM mass flow rate predictions (orange line) and experimental measurements (blue line) in the three API experiments for which tabulated data exists. The top row of Figure 9 shows comparisons corresponding to the 168 mm internal diameter pipe at 71 bar (left) and 36 bar (right), the bottom row shows the comparisons for the 300 mm internal diameter pipe case. In all cases, the GasPiRRaM model makes qualitatively reasonable predictions. GasPiRRaM makes significantly larger predictions of the initial mass flow rate, but the duration of these is very short and may have been beyond the measurement capability at the time. It is also useful to note that the uncertainty in the experimental measurements is not reported. As such it is difficult to make meaningful inferences in the later stages of the releases where it appears that the model under predicts the experimental data.

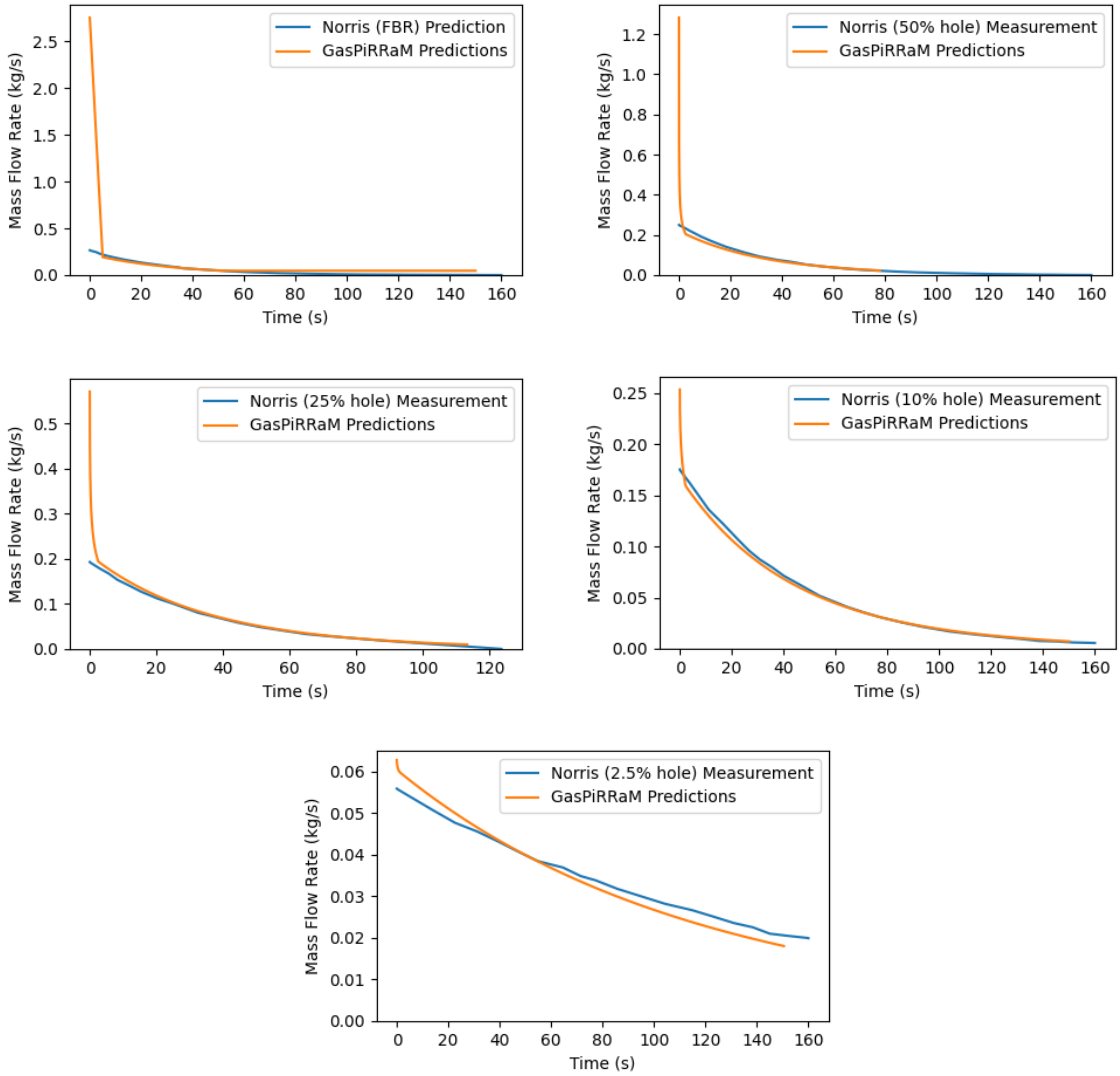

Figure 8 Comparison of the transient mass flow rate predicted by GasPiRRaM to the experimental measurements of Norris and Puls (1993) for the case of a full bore rupture (top left); a 50% of the pipe area hole (top right); a 25% of the pipe area hole (middle left); a 10% of the pipe area hole (middle right); and a 2.5% hole (bottom row). GasPiRRaM predictions are shown using orange lines, and experimental measurements are shown using blue lines.

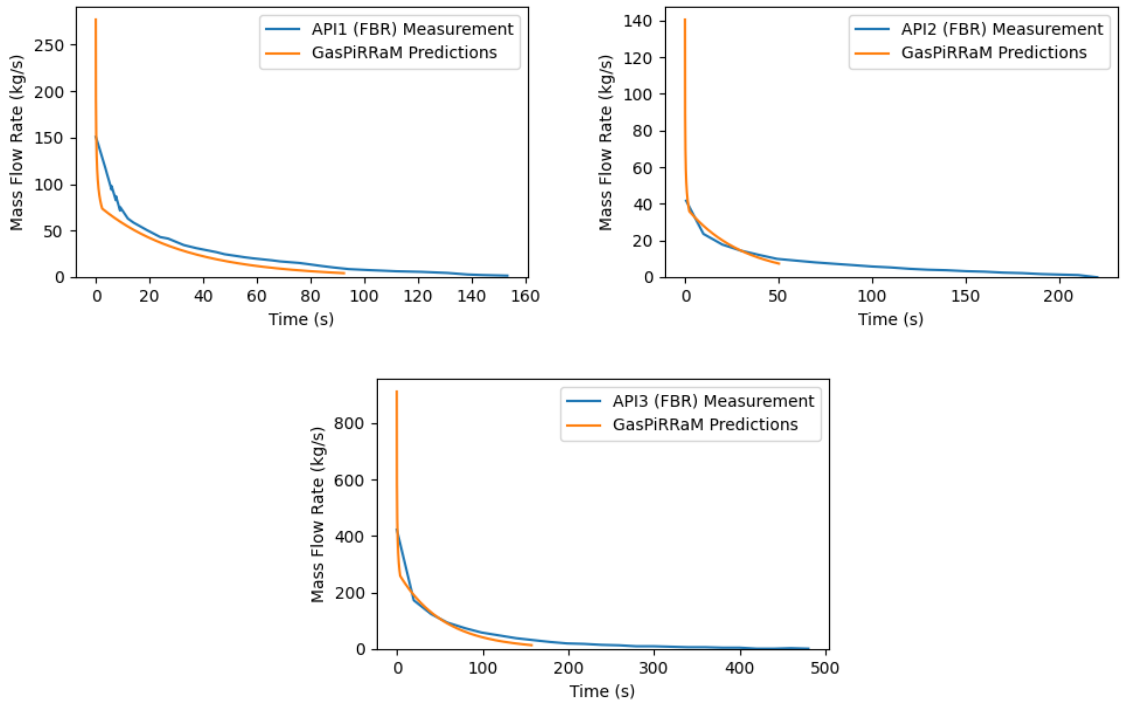

Figure 9 Comparison of the transient mass flow rate predicted by GasPiRRaM to the experimental measurements of the Alberta Petroleum Institute for the case of a full bore rupture in a 2 km long, 168 mm diameter pipe (top row), and a 3.5 km long, 305 mm diameter pipe (bottom row). GasPiRRaM predictions are shown using orange lines, and experimental measurements are shown using blue lines.

8.3 Botros *et al.* (1989) Experiments

Botros et al. (1989) present measurements from field experiments performed by the Nova Corporation of Alberta Field (NCAF). These relate to the depressurisation of a 25.5 km long, 203 mm diameter pipeline containing a natural gas mixture through a vent stack with a cross-sectional area that is 25% of the main pipeline into a 17% orifice. The initial pressure and temperature of the pipeline were 40.9 bar and 292 K, respectively. GasPiRRaM models this experiment using pure methane as the working fluid, with the parameters given in Table 7, which ignore the vent stack prior to the orifice.

Table 7 GasPiRRaM model input parameters corresponding to the Botros *et al.* (1989) dataset

Material	D_{pipe}	D_{hole}	$A_{\mathrm{hole}}A_{\mathrm{pipe}}^{-1}$	L_{pipe}	P_0	T_o	μ
Methane	203 mm	83.5 mm	17 %	25.52 km	40.9 bar	292 K	45 um

Figure 10 shows a comparison of GasPiRRaM exit pressure predictions (orange line) and experimental measurements (blue line) for the Botros (1989) experiment. The agreement between the model predictions and experimental data is qualitatively very reasonable. The model generally underpredicts the experimental data, but as the experimental uncertainties are not reported, it is not possible to comment definitively as to whether the underprediction is reasonable. The generally good level of agreement between the model prediction and the experimental data indicates that the model is working acceptably well for HSE's intended purpose.

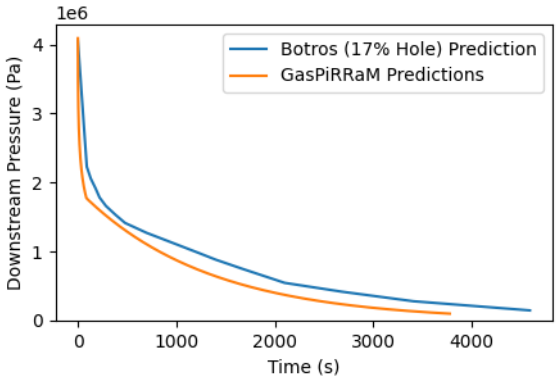

Figure 10 Comparison of the transient downstream pressure predicted by GasPiRRaM to the experimental measurements reported in Botros *et al.* (1989) for the case of a 17% hole in a 25.5 km long, 200 mm diameter pipe. GasPiRRaM predictions are shown using orange lines, and experimental measurements are shown using blue lines.

9 Discussion

This paper reports on HSE's new GasPiRRaM model that predicts the transient characteristics of gas pipeline decompression for use in HSE's MISHAP pipeline risk tool. The new model is derived using key elements of the PolyPiRRaM model combined with the slowly evolving flow technique adopted in HSE's PiRRaM and DNV PHAST's GasPipe models. The model is verified to analytical solutions, compared to other tools and validated to the available experimental data. Across this range of comparisons, GasPiRRaM is shown to work well and perform acceptably, without any obvious weaknesses or limitations. GasPiRRaM does predict larger initial mass flow rates in comparison to DNV's GasPipe model and the experimental measurements of Norris, but these are believed to be due to the slight differences in modelling, and the approach taken to analyse the experimental data. The model is shown to smoothly transition between the PolyPiRRaM full-bore rupture model and the exponentially decaying vessel model. The model can be run for arbitrarily small hole sizes without restriction.

In testing GasPiRRaM, a new non-dimensionalisation has been found that enables a re-interpretation of the PolyPiRRaM full bore rupture model and provides a route to generalise that approach to hole type releases. Newton (2025) explores this option demonstrating that the PolyPiRRaM calculation can be extended to precisely replicate GasPiRRaM, and provides acceptable approximation to PiRRaM for saturated liquid releases (Newton, 2022).

Authorship

The author confirms sole responsibility for the following: study conception and design, data collection, analysis and interpretation of results, and manuscript preparation.

Acknowledgements

The author gratefully acknowledges Zoe Chaplin and Simon Coldrick of HSE, and Gemma Tickle of GT Science &and Software Ltd, for their editorial and technical comments which have helped improve the manuscript.

Disclaimer

This publication and the work it describes were funded by the Health and Safety Executive (HSE). Its contents, including any opinions and/or conclusions expressed, are those of the authors alone and do not necessarily reflect HSE policy.

10 References

APIGEC. (1979). Hydrogen Sulphide Isopleth Prediction, Phase 2, Pipe Burst Study. *A report by Alberta petroleum industry government environmental committee.* .

Bell, I. H., Wronski, J., Quoilin, S., & Lemort, V. (2014). Pure and pseudo-pure fluid thermophysical property evaluation and the open-source thermophysical property library CoolProp. *Industrial & engineering chemistry research*, *53*(6), 2498-2508.

Bell, R. (1978). Isopleth calculations for ruptures in sour gas pipelines. *Energy Processing/Canada*, *36*.

Bendlksen, K. H., Malnes, D., Moe, R., & Nuland, S. (1991). The dynamic two-fluid model OLGA: Theory and application. *SPE production engineering*, *6*(02), 171-180.

Betteridge, S. (2023). *Shell FRED 2023 Technical Guide Technical description of hazard consequence models (Fire, Release, Explosion, Dispersion) in FRED* (INTERNAL – SRN--04582). Shell Research Limited.

Botros, K., Jungowski, W., & Weiss, M. (1989). Models and methods of simulating gas pipeline blowdown. *The Canadian Journal of Chemical Engineering*, *67*(4), 529-539.

Eiber, R., Bubenik, T., & Maxey, W. (1993). *Fracture control technology for natural gas pipelines*. Technical Toolboxes, Incorporated.

Fannelop, T., & Ryhming, I. (1982). Massive release of gas from long pipelines. *Journal of Energy*, *6*(2), 132-140.

Haaland, S. E. (1981). *Simple and Explicit Formulas for the Friction Factor in Turbulent Pipe Flow, Including Natural Gas Pipelines*. Univ., Norwegian Inst. of Technol., Division of Aero-and Gas Dynamics.

Maxey, W. (1974). Fracture initiation, propagation, and arrest. Proc. of Symposium on Line Pipe Research, 1974,

Newton, A. (2022). Pipeline Release Rate Model for pressure liquedifed flows. *Hazards 32, Symposium Series*. https://www.researchgate.net/publication/365623566_Pipeline_Release_Rate_Model_PiRRaM_for_Pressure_Liquefied_Gases

Newton, A. (2024). *An Analytical Solution to the Transient One-Dimensional Compressible Pipe-Flow Equations* Hazards 34, Symposium Series, Manchester. https://www.researchgate.net/publication/384599390_An_Analytical_Solution_to_the_Transient_One-Dimensional_Compressible_Pipe-Flow_Equations

Newton, A. (2025). PolyPiRRaM+: A Simple Universal Model of Compressible Pipeline Failure. *Hazards 35, Symposiuym Series*.

Norris, H., & Puls, R. (1993). Single-phase or multiphase blowdown of vessels or pipelines. SPE Annual Technical Conference and Exhibition?,

Richardson, S., & Saville, G. (1991). Blowdown of pipelines. SPE Offshore Europe Conference and Exhibition,

Webber, D., Fannelop, T., & Witlox, H. (1999, September). Source terms from two-phase flow in long pipelines following an accidental breach. International Conference and Workshop on Modelling the Consequences of Accidental Releases of Hazardous Materials, CCPS, San Francisco, California.

Weiss, M., Botros, K., & Jungowski, W. (1988). Simple method predicts gas-line blowdown times. *Oil Gas J.;(United States)*, *86*(50).

Wilson, D. J. (1979 (Re-issued 1986)). Release and Dispersion of Gas from Pipeline Ruptures.pdf. *Alberta Environment*.

Worthington, D. (2022). Theory, GasPipe. *DNV Technical Documentation*. https://mysoftware.dnv.com/download/public/phast/technical_documentation/03_discharge/long_pipeline_model/Gaspipe%20Model%20Theory.pdf

11 Terminology and Nomenclature

11.1 Nomenclature

Parameter	**Description**	**Units**
A	Area	m^2
D	Diameter	m
G	Mass flux density	kg m^{-2} s^{-1}
L	Pipe length	m
P	Pressure	Pa
$\dot{M}$	Mass flow rate	kg s^{-1}
M	Pipe inventory	kg
R	Gas constant	J $mol^{-1}K^{-1}$
T	Temperature	K
f	Fanning friction factor - Haaland correlation (Haaland, 1981)	-
m	Polytropic index	-
n	Pipe exponent (n=2, gas)	-
t	time	s
B_z	Incomplete beta function	-
γ	Ratio of specific heats	-
ρ	Fluid density	kg m^{-3}
$\lambda, \mu, \psi, \omega$	Dimensionless constant	-
μ	Pipe surface roughness	m

11.2 Subscripts

Subscript	Explanation
dw	Downstream end of the pipe
expd	Referring to the expanding zone
i	Integer index
pipe	Referring to the pipe
trans	Conditions at the transition between choked and unchoked flow regimes
up	Upstream end of the pipe
0	Initial conditions